ORIGINAL RESEARCH

Effect of various geopolymerization parameters on poor quality Afşin-Elbistan fly ash-based geopolymer concretes with ground granulated blast furnace slag

Ahmet Hayrullah Sevinç[1] · Muhammed Yasin Durgun[2]

Abstract

The utilization of Afşin-Elbistan fly ash (FA), which cannot be used in cement and concrete industry in production of geo-polymers, has been studied with some preliminary trials. In this study, FA of Afşin-Elbistan thermal power plant, which does not fit any of FA classes according to ASTM C 618, was used as a geopolymer binder raw material. The main motivation of the study is to investigate the partial usability of this type of FA, which is not sufficient on its own and creates a large amount of waste, as a geopolymer raw material. FA was replaced with ground granulated blast furnace slag (GGBFS) by the ratios of 25% and 50% (by weights) in order to develop the properties of geopolymer concrete. Sodium silicate (SS) and sodium hydroxide (SH) (10 and 14 M) were used as activators. Three different activator to binder ratios (0.45, 0.55 and 0.65) and three SS/SH ratios (0.75, 1.0 and 1.5) were chosen. Unit weight, compressive strength, splitting tensile strength, and ultra-sonic pulse velocity tests were performed for 28 and 60 days. In order to investigate the microstructure, scanning electron microscopy (SEM) analyses were performed. As a result, GGBFS incorporation enhanced the properties of Afşin-Elbistan FA-based geopolymer concrete. With the increase of GGBFS content, the compressive strength values increased. The highest strengths were obtained from 50% GGBFS groups. The results revealed that Afşin-Elbistan FA (AEFA), which has the high-est waste reserve among the thermal power plant fly ashes in Turkey, could be evaluated as partial geopolymer raw material.

Graphical abstract
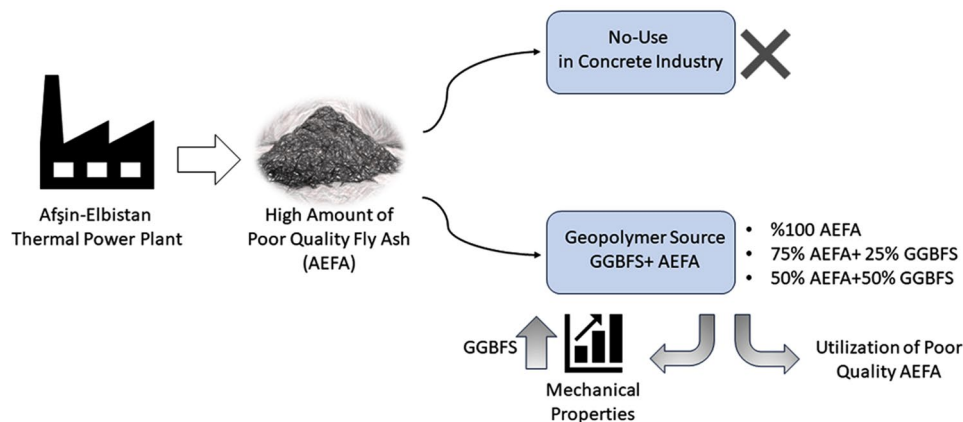
Extended author information available on the last page of the article

Springer

Introduction

Global warming and climate changes are serious threats for all biological organisms. Gases like methane, nitrous oxide and carbon dioxide, which are called greenhouse gases, have led to environmental hazards. It is known that concrete is the most common construction material around the world [1]. Cement is one of the main constituents of concrete. However, the cement production process has some drawbacks for the environment such as CO_2 emissions. It was reported that the cement industry is responsible for 5–7% of the total CO_2 emission in the world [2]. Hence, it is necessary to reduce CO_2 emission to the atmosphere. This reduction can be obtained by facing new binder materials or new techniques except for conventional cement production [3].

Geopolymer has been investigated since Davidovits used this term in 1978 [4]. It can be also named as low-temperature aluminosilicates [5], alkali-activated cements [6], alkali-bonded ceramics [7], inorganic polymeric concretes [8], and hydroceramics [9].

Geopolymer concrete is a cement-free material. Therefore, it is often called "green concrete". Industrial by-products such as blast furnace slag, fly ash, and silica fume are commonly used as geopolymer concrete raw materials instead of cement. Geopolymer concrete not only reduces the CO_2 emission through cement production but also reduces the waste materials of the industrial processes [10]. These industrial waste materials generally constitute the aluminosilicate sources for the geopolymerization reaction [11–13] such as fly ash (FA) and ground granulated blast furnace slag (GGBFS) [14]. The aluminosilicate sources can be obtained also naturally such as clays, red mud, and metakaolin [15]. Besides nano-materials such as nano-silica have been used recently for the modification of geopolymer concrete [16]. These materials are needed to be activated by an alkaline activator solution such as sodium or potassium hydroxide and sodium silicate [11].

The most suitable industrial by-product for geopolymerization is FA. It is produced in huge amounts every year by the thermal power plants and collected by the mechanic and the electrostatic filters [17]. It consists of amorphous silica and alumina. The size and the shape of this material increase the workability and this makes FA suitable for geopolymer concrete production [18, 19]. Sometimes the main aluminosilicate source FA can be partially replaced by GGBFS or other fines [16] in order to develop the properties of FA-based geopolymer concrete [20–22]. It was reported that GGBFS incorporation in the FA-based geopolymer concrete reduced the setting time and workability and increased the compressive strength.

In the literature, the effects of various geopolymerization parameters on the properties of geopolymer concrete were investigated [23]. These parameters are generally curing conditions [24–26], molarity of activator solution [27, 28], and activator/binder ratio (Ac/B) [8, 29, 30]. Niş and Altındal [31] subjected geopolymer mixtures containing different amounts of FA and GGBFS to 13 different curing types. These include laboratory, oven, and water environments, temperatures, and application times. The study's results showed that increasing the curing time increased the compressive strength. In the samples produced with GGBFS, the best results were obtained from the sample kept in the oven at 70 °C for two days and in water for 26 days. The worst results were obtained from the sample kept in the air for 26 days and in the oven for two days. When the molarity of the activator used is examined, it is seen that concentrations between 8–14 M are preferred in GGBFS-based mixtures [32]. While it was reported that the increase in Na_2O/SiO_2 ratio had positive results on compressive strength, it was stated that increasing the amount of alkaline solution in the mixture negatively affected the strength [33, 34]. On the other hand, a study comparing 8, 12, and 16 M solutions stated that the increase in molarity increased splitting and bending strength [35].

Afşin-Elbistan thermal power plant (a coal-burning power plant in Kahramanmaraş region in Turkey) FA (AEFA) was used as the main aluminosilicate source for the geopolymer. This AEFA does not fit any of the FA classes according to ASTM C 618. The total amount of SiO_2, Al_2O_3, and Fe_2O_3 is lower than 50% and the amount of SO_3 is high. Therefore, it cannot be utilized in the concrete industry conversely to other FA types in Turkey. Besides, this thermal power plant has the highest energy generator and the highest FA production in the country [36]. The cement and concrete industry is the safest sector to use FAs, but this situation for AEFA causes a huge amount of FA remains as waste. AEFA, which cannot be used in the concrete industry due to its chemical composition and non-standard nature, has been evaluated in many ways by researchers and tried to be brought to the industry. For this purpose, its usability in various forms of cementitious composites (shrinkage reducer, etc.) [37–39], in soil improvement and stabilization [40, 41], glass production [42], building materials such as bricks and briquettes [43], its use in light-weight building material production [44], and chipboard production [45] has been investigated. Only a few studies have been done on its use in geopolymers and alkali-activated materials. In these studies, it is observed that the use of AEFA has negative results in mechanical properties or that it only produces acceptable results when used with a component such as silica fume at a rate of up to 25% [46, 47]. In another study conducted by the authors, the use of a certain amount of silica source (glass powder and silica fume) and the evaluation of AEFA in

geopolymer systems were investigated. In this way, the use of hybrids has provided partially effective results [48]. In another study, it was used with GGBFS, similar to this study. Here, a value as low as 6 MPa could be obtained [49]. The difference that distinguishes this study from the current study is that it does not contain chemical activators.

The usability of AEFA, which cannot be used in the cement and concrete industry, in the production of geopolymers has been investigated with some preliminary trials. However, when compared with the strength values of geopolymers produced with FA in the literature, it was seen that AEFA resulted in significantly lower results. These findings have led to the idea that AEFA is not suitable for use as a geopolymer raw material. In the "Results and discussion" section, the results obtained from the samples produced with 100% AEFA are also given as reference values. The main purpose of this study is to examine the evaluability of AEFA, which is insufficient on its own, by using it as a hybrid with another geopolymer raw material (GGBFS). Thus, it is aimed that AEFA can be partially evaluated in geopolymer production. In this context, AEFA was replaced by 25% and 50% with GGBFS, and sodium hydroxide (SH) and sodium silicate (SS) were chosen as the activators. In order to determine the effects of geopolymerization parameters on the properties of geopolymers SS/SH ratio, the molarity of SH and activator to binder ratio (Ac/B) were changed. Unit weight, compressive strength, splitting tensile strength, and ultrasonic pulse velocity tests were performed on geopolymer concretes at different curing ages. Besides, the microstructures of the mixtures were investigated by scanning electron microscopy (SEM).

Experimental

Materials

The FA used in the study was obtained from the Afşin-Elbistan thermal power plant in the Kahramanmaraş region. The GGBFS used in the study was obtained from Iskenderun Steel and Iron Factory. Physical and chemical properties of AEFA and GGBFS were determined by X-ray fluorescence (XRF) analysis and given in Table 1 and the XRD patterns of the materials are given in Fig. 1. The SEM images of materials are given in Fig. 2. In the study, calcareous coarse aggregates with 8 mm maximum grain size and 0–4 mm crushed sand were used. The specific gravities of coarse and fine aggregate are 2.78 and 2.71, respectively.

As activators commercially obtained Na_2SiO_3 and NaOH solutions were used. Properties of sodium silicate are given in Table 2.

Table 1 Physical and chemical properties of AEFA and GGBFS

| Compounds (%)	AEFA	GGBFS
Chemical analysis results		
SiO_2	22.73	44.31
Al_2O_3	9.67	10.07
Fe_2O_3	4.63	1.43
CaO	42.94	31.18
MgO	1.99	8.54
SO_3	9.01	–
$Na_2O + K_2O$	0.83	–
Loss on ignition	5.21	–
Physical analysis results		
Specific gravity	2.42	2.88
Fineness (cm^2/g)	2200	5500

Mix design

The mixture series are given in Table 3. GGBFS was used instead of AEFA by the ratios of 25% and 50% by weights. As alkaline liquid, SH and SS solutions were used. SH was obtained as commercial flakes and the SH solution was prepared with distilled water with 10 and 14 molar concentrations. SS is commercially obtained as liquid. The ratio of SS/SH was selected as 0.75, 1.0, and 1.5. Three different Ac/B ratios were selected, which were 0.45, 0.55, and 0.65. 81 different mixture series were produced according to the selected geopolymerization parameters (Table 3). In the figures, three main codes were used. These are "FA" for 100% AEFA-containing samples, and "S25" and "S50" for 25% and 50% GGBFS-containing samples, respectively. Also, codes have numbers according to Ac/B and SS/SH amount. For example, S50-0.65/1.5 indicates the sample with 50% GGBFS, 0.65 Ac/B, and 1.5 SS/SH.

Production of samples

Due to its exothermic nature, the SH solution was prepared the day before the production of geopolymer concrete. Aggregates and the raw materials (AEFA and GGBFS) were dry mixed in a laboratory-type mixer for 3 min. SH and SS solutions were mixed and this liquid mixture was poured on the dry mixture and was mixed for another 4 min. Fresh mixtures were cast into $50 \times 50 \times 50$ mm molds and compacted using a vibration table. Fresh mixtures were cured in a laboratory oven at 85 °C for 24 h. Preliminary trials showed that the fresh mixtures could not be set at room temperature in a sufficient time. Therefore, heat curing was applied. After the heat curing, samples were demolded and kept at 20 ± 2 °C and $60 \pm 5\%$ relative humidity for 28 and 60 days.

Fig. 1 XRD patterns of materials: **a** AEFA, and **b** GGBFS (A: Anhydrite, C: Calcite, Q: Quartz, Al: Alumina, L: Lime)
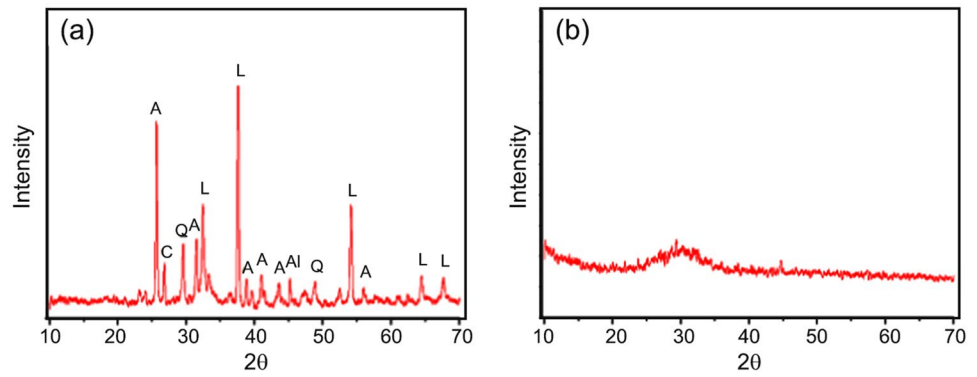
Fig. 2 SEM images of materials **a** AEFA, and **b** GGBFS
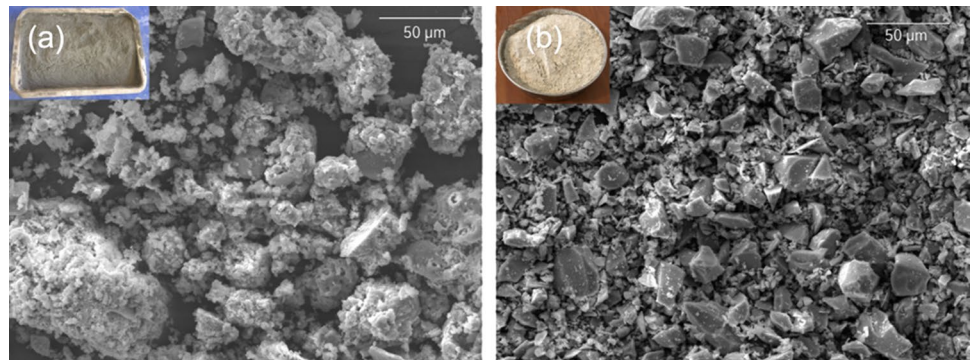
Table 2 Properties of sodium silicate

| Parameter	
Appearance	Clear liquid
Origin	Alkali sand
SiO_2 (%)	22.56
Na_2O (%)	10.94
Module (SiO_2/Na_2O)	1.94
Béº	38
Density (g/cm³ at 20 °C)	1.37
Viscosity (cP at 20 °C)	115

Testing procedure

Fresh and hardened unit weights of mixtures were tested. Ultrasonic pulse velocity (UPV) tests were performed on the samples according to ASTM C 597. After the UPV test, the uniaxial compressive strength test (TS EN 12390-3, 2010) and splitting tensile strength test (TS EN 12390-6, 2010) were performed on the samples at 28 and 60 days. Figure 3 shows various images from the experimental study.

Table 3 Mixture series according to the selected geopolymerization parameters

Ac/B		100% FA			75% FA + 25% GGBFS			50% FA + 50% GGBFS		
		0.45	0.55	0.65	0.45	0.55	0.65	0.45	0.55	0.65
10 M	SS/SH	0.75	0.75	0.75	0.75	0.75	0.75	0.75	0.75	0.75
		1.00	1.00	1.00	1.00	1.00	1.00	1.00	1.00	1.00
		1.50	1.50	1.50	1.50	1.50	1.50	1.50	1.50	1.50
14 M		0.75	0.75	0.75	0.75	0.75	0.75	0.75	0.75	0.75
		1.00	1.00	1.00	1.00	1.00	1.00	1.00	1.00	1.00
		1.50	1.50	1.50	1.50	1.50	1.50	1.50	1.50	1.50

Fig. 3 Images from experiments: **a** oven curing, **b** heat-treated samples, **c** UPV test, and **d** compressive strength test
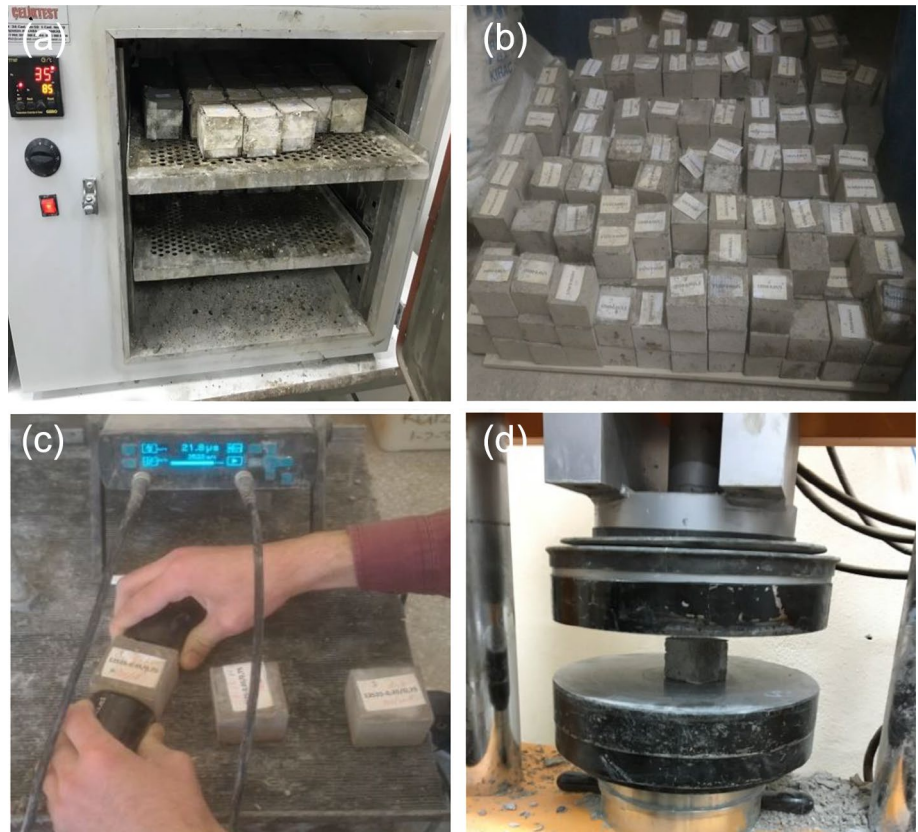
**Fig. 4** Fresh and hardened unit weight of 10 M SH containing samples
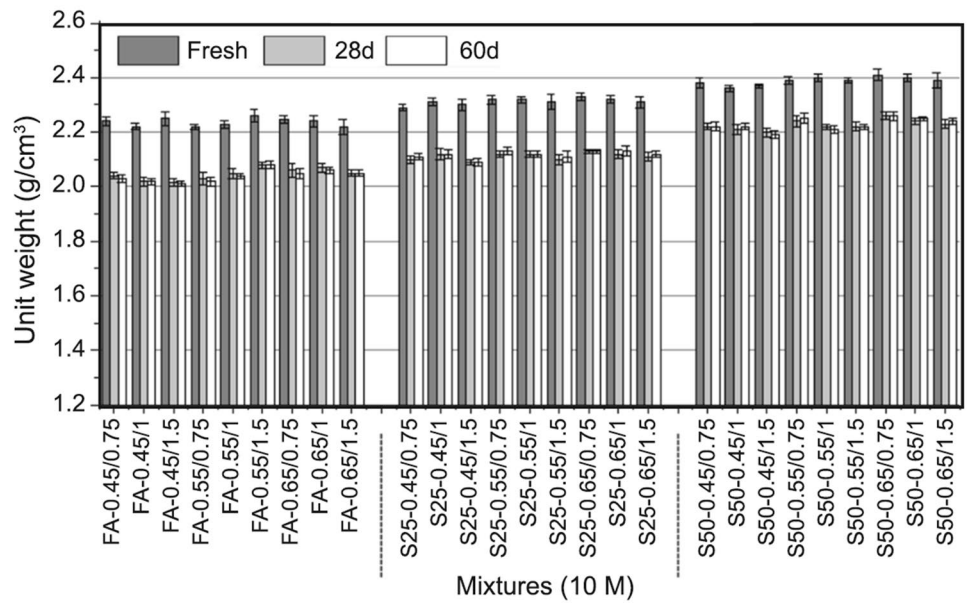
Results and discussion

Fresh and hardened unit weight

The fresh and hardened unit weight results are given in Figs. 4 and 5. The fresh unit weight values of the mixtures varied between 2.22–2.41 g/cm^3. The fresh unit weights of the mixtures increased with increase of GGBFS content. For a conventional hardened concrete, unit weight generally changes between 2.3–2.5 g/cm^3 [50, 51]. The unit weights of 100% AEFA-containing hardened sample

**Fig. 5** Fresh and hardened unit weight of 14 M SH containing samples
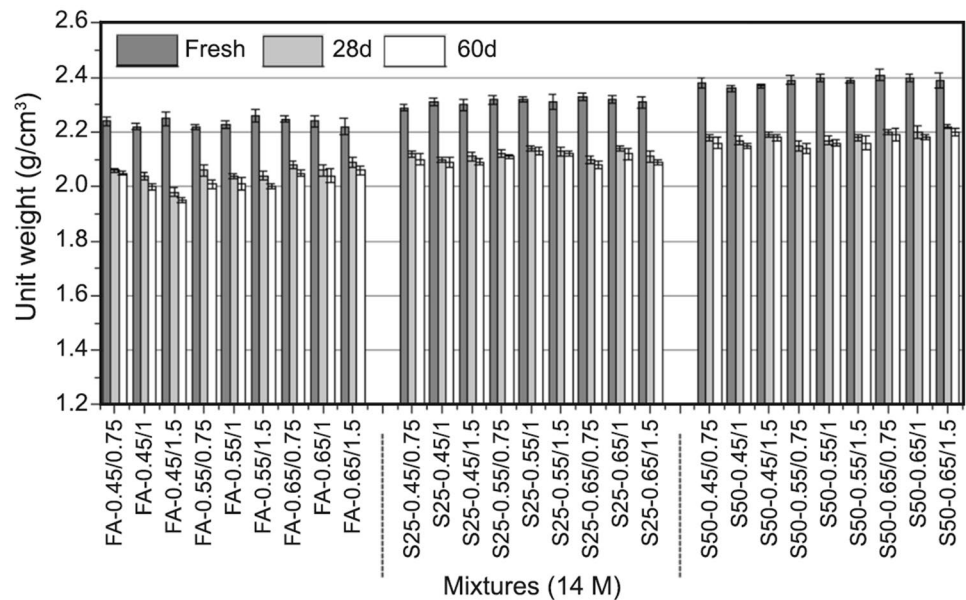
group changed between 1.98–2.09 g/cm³, for both ages and molarities. 25% GGBFS-containing sample groups have shown unit weight values between 2.09–2.14 g/cm³. This range is 2.14–2.26 g/cm³ for 50% GGBFS-containing group. It is seen that GGBFS-containing groups have higher unit weight values than 100% AEFA-containing groups and they have given more similar results to conventional concrete. According to the results, geopolymer concretes produced completely with AEFA are lighter than slag-containing samples. These results can be related to the higher specific gravity of the GGBFS compared to AEFA (Table 1). One other possible reason is the degree of geopolymerization reactions of the samples containing GGBFS. An increase in the degree of the reaction also means more reaction products and less pores. From Figs. 4 and 5 it is possible to conclude that the results of the unit weight tests were not significantly affected by the concentration of SH, Ac/B, and the age of the samples.

Ultrasonic pulse velocity test results

UPV test results are given in Figs. 6 and 7. UPV strongly depends on the pore structure and density of the material. Hence, there is a strong relationship between the mechanical properties and the UPV results [52].

In the series containing 10 M SH for 28 day samples, the UPV value varied between 1266–1613 m/s in the samples containing only AEFA, while adding 25% GGBFS increased this range to 1493–2565 m/s. 50% GGBFS addition increased this range to 2033–3049 m/s. In the 60-day series, these values were slightly higher and the range of all samples was 1275–3368 m/s. In the series containing 14 M SH, 60 day samples containing only AEFA gave a
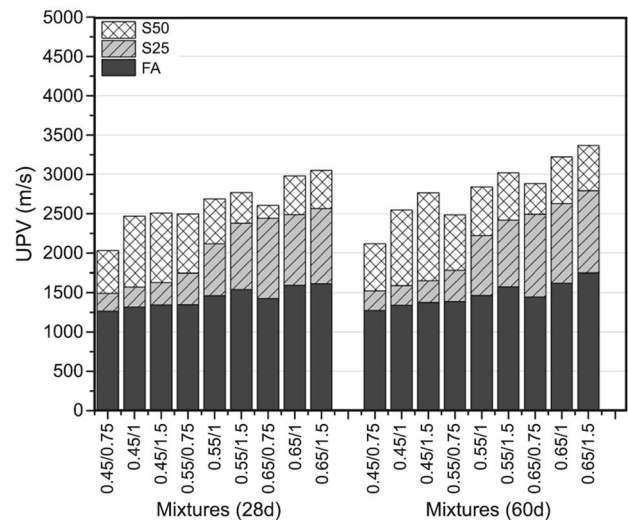
Fig. 6 UPV values of 10 M SH containing samples

range of 2475–3029 m/s, samples containing 25% GGBFS 2561–3884 m/s, and samples containing 50% GGBFS gave a range of 2794–4581 m/s. It is seen that the 60-day samples have slightly higher values than the 28 day samples. The lowest UPV result was obtained from the 100% AEFA sample with 10 M SH, 0.45 Ac/B ratio, and 0.75 SS/SH ratio. The highest result was obtained from the 50% FA sample with 14 M SH, 0.65 Ac/B ratios, and 1.50 SS/SH ratio. According to the UPV results, GGBFS-containing samples have higher UPV results. For example, the addition of GGBFS to samples containing only AEFA in 60 day samples resulted in an increase from 11 to 101%. The UPV results also increased with the increase of SS/SH ratio. The
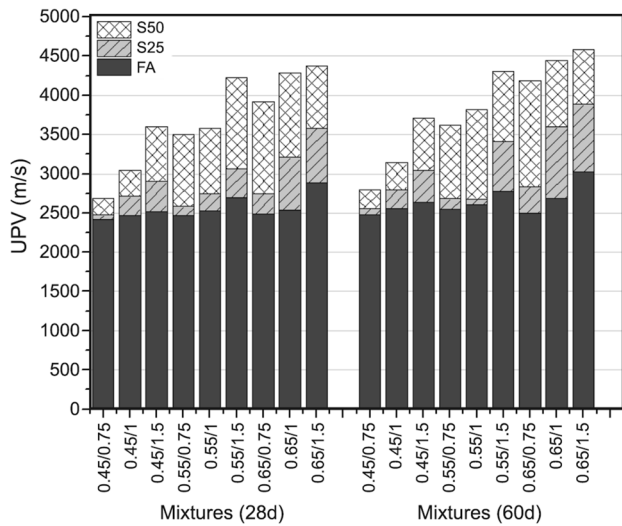
Fig. 7 UPV values of 14 M SH containing samples

increase in SS/SH ratio from 0.75 to 1.5 provided an increase between 6.6% and 37% for the same sample group. Another parameter that improves the results is the increase in the Ac/B ratio. Increasing the Ac/B ratio from 0.45 to 0.65 in the same sample group increased the results between 1 and 69%. In addition, the increase in SH concentration was also effective in increasing the UPV values. The increase in SH concentration from 10 to 14 M in 60 day samples resulted in an increase between 13 and 94%. As mentioned before, it is known that there is a strong relationship between mechanical properties and UPV [52]. Therefore, it can be said that the parameters affecting variations in UPV and the mechanical

properties are similar. The reasons for the variation in results are therefore discussed in the next section.

Compressive strength results

Compressive strength test results are given in Fig. 8. According to the 28 day compressive strength results, for mixtures produced with 100% AEFA and 10 M SH, the lowest result is 2.52 MPa and the highest result is 5.63 MPa. The increment is 123% with the increase of SS/SH and Ac/B ratio. When 14 M SH was used, the lowest strength increased to 2.66 MPa and the highest value increased to 6.85 MPa. The increment in strength between is 157.5%. The lowest value was obtained as 4.47 MPa and the highest as 12.69 MPa when 25% of GGBFS was used in the mixture with 10 M SH. The strength increment in the 10 M group is 184%. The highest value of 100% AEFA-containing group (10 M-0.65/1.5–5.63 MPa) increased to 16.42 MPa with 50% GGBFS addition. The increment is 191.7%.

When the molarity increased to 14 M, the lowest strength value increased to 9.35 MPa and the highest value increased to 30.57 MPa. The highest value of 100% AEFA-containing group is 15.26 MPa (14 M-0.65/1.5). This value increased to 30.57 MPa by 50% GGBFS addition. The increment is 100.3%. It can be seen that the compressive strength of samples significantly increases by the addition of GGBFS. In the literature, it is reported that GGBFS addition into fly ash-based geopolymer mixtures increases the compressive strength. This is associated with the rapid reaction of very fine GGBFS particles and alkaline solutions. This reaction mainly forms hydrated phases such as calcium silicate hydrates (C–S–H) and calcium–aluminum–silicate–hydrate
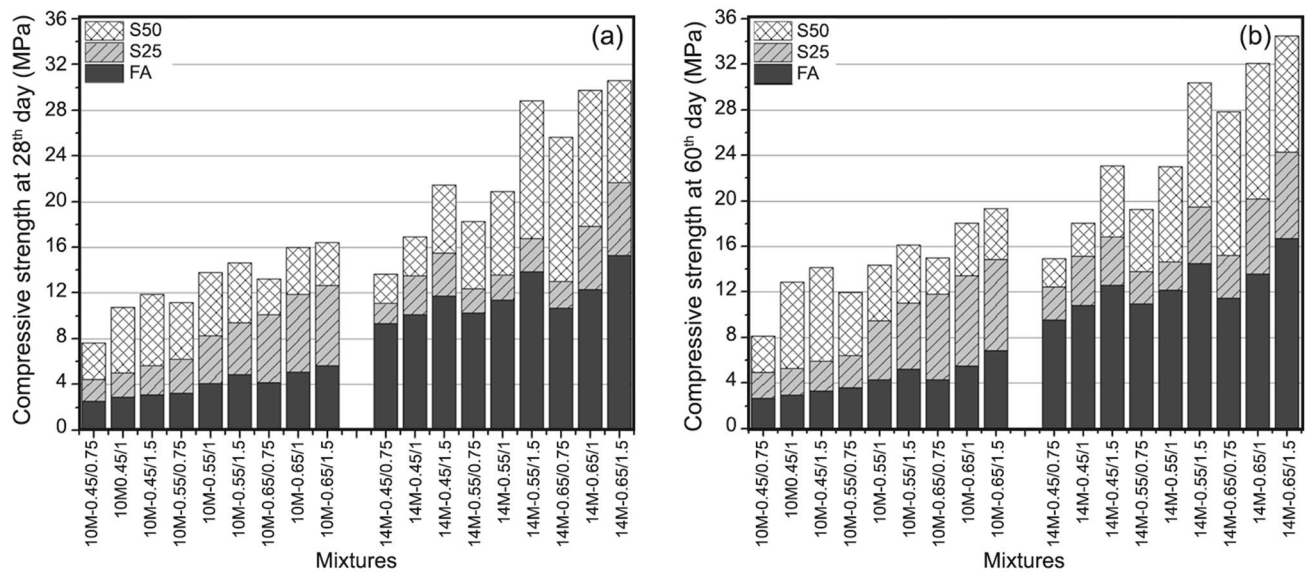

Fig. 8 Results of compressive strength test: **a** 28 day, and **b** 60 day

gels (C–A–S–H) and contributes to the compressive strength of the material [53–55]. On the other hand, the GGBFS used in the study has finer grains compared to the fly ash. This increases the specific surface area and results in an increment in the reactivity of the mixture.

On the other hand, it was observed that the increase in the SS/SH ratio increased the compressive strength of the AEFA-based samples. The highest values in the groups were obtained from the 1.50 SS/SH ratio. The increment range in the compressive strength with the increase of SS/SH ratio from 0.75 to 1.5 in 100% AEFA series is 23.4–49.8%, for 25% GGBFS group is 25–65.8% and for 50% GGBFS group is 19.2–57.6% in 28 day tests. In 60 day tests, these values are 23.3–60%, 21.3–71.7% and 23.9–73.7%, respectively.

At all mixture series the compressive strength results were increased with the increase of Ac/B ratio. 0.65 is the highest strength giving group in different Ac/B ratios. In 28 day results, for 100% AEFA-containing group the strength increment range with the increase of Ac/B ratio from 0.45 to 0.65 is 13.9–81%, for 25% GGBFS group 17.9–136.5% and for 50% GGBFS group 37.8–87.4%. For 60 day tests these results are 20–108.8%, 22.1–155.2% and 36.4–86.5%, respectively.

The increment in the Ac/B ratio leads to a better dissolution of the aluminosilicate ions. In this way, it became possible to produce more reaction products [56]. Moreover, reaction kinetics and stability are known to be affected by the Ac/B ratio. In addition, it has been stated in the literature that the increase in sodium concentration in the activator solution increases the ionic strength and provides better deflocculation of anhydrated GGBFS grains [55]. Besides, the increase of SS/SH ratio provides sufficient SS for the geopolymerization reactions and this leads to an increment in the formation of the geopolymeric gel [57, 58]. It is reported that SS usually leads to the highest mechanical properties [59].

The increase in SH concentration appears to have a serious effect on the results. When the 28 day results are examined, the minimum increase obtained by increasing the molarity from 10 to 14 M in the samples produced using AEFA alone is 143.5%, while the highest is 277.8%. These values were 28.7% and 175.7%, respectively, in the group containing 25% GGBFS, and 51.7% and 96.5%, respectively, in the group containing 50% GGBFS. The increment values of the 60 day samples are very close to the 28 day increase values. High NaOH concentration increases the alkalinity of the activator solution. This accelerates the dissolution of Si and Al ions and causes an increase in the amount of hydration products [58].

It can be said that the curing time does not have a very serious effect on the results. The increase in compressive strength between 28 and 60 days in the sample group containing 10 M SH ranged from 2% to 21.7%, while the same rate varied from 2% to 16.4% for the groups containing 14 M SH.

Relationship between UPV and compressive strength

The relationships between UPV and compressive strength are shown in Figs. 9 and 10. From Fig. 9 it can be seen that there is a good relationship between UPV results and the compressive strength results of the geopolymer concretes at 28 days. As response parameters, the compressive strength values were considered and UPV results were taken as predicted factors. A linear regression method was used and very high R^2 values were obtained, which are between approximately 0.93 and 0.99. This means there is a good correlation between UPV and compressive strength results. The linear regression equations can be seen in the figures.

Figure 10 shows the relationship between UPV and compressive strength at 60 days. There can be seen a good correlation similar to 28 day results. The determination coefficients (R^2) were also between approximately 0.93 and 0.99.

The porosity of the material and the cracks in the structure directly affect the UPV results. High amounts of cracks and high porosity lead to lower UPV values. It is known that the UPV results of the mixtures indicate mechanical properties such as compressive strength, flexural strength, and elastic modulus [60, 61].

Splitting tensile strength results

The splitting tensile strength test results are given in Fig. 11. According to the splitting tensile strength results at 28 day, for 100% AEFA-containing geopolymers with 10 M SH, only two samples gave results. It was not possible to read a strength value from the other seven series. The obtained values are 1.22 and 1.31 MPa. 14 M SH group results vary from 1.92 to 2.89 MPa. 25% GGBFS-containing group has results between 1.22 and 2.77 MPa for 10 M SH and 2.24 and 3.91 MPa for 14 M SH. 50% GGBFS-containing group has shown the highest values which are between 1.67 and 3.16 MPa for 10 M and 2.62 and 4.97 MPa for 14 M.

At 60 day tests, the highest value was obtained from 14S50-0.65/1.5 again as compressive strength and the value is 5.36 MPa. The lowest value was obtained from 10S25-0.45/0.75. The result is 1.15 MPa. However, from Fig. 11b, it should be taken into account that strength values could not be obtained from most of the samples produced using only AEFA.

The highest values were obtained from 1.50 SS/SH. The results increased with the increase of this ratio. For 28 day results, according to SS/SH ratio change, the highest strength increment in the 10 M group for 25% and 50% GGBFS are 45.1%, 53.9%, respectively. Adequate results could not be
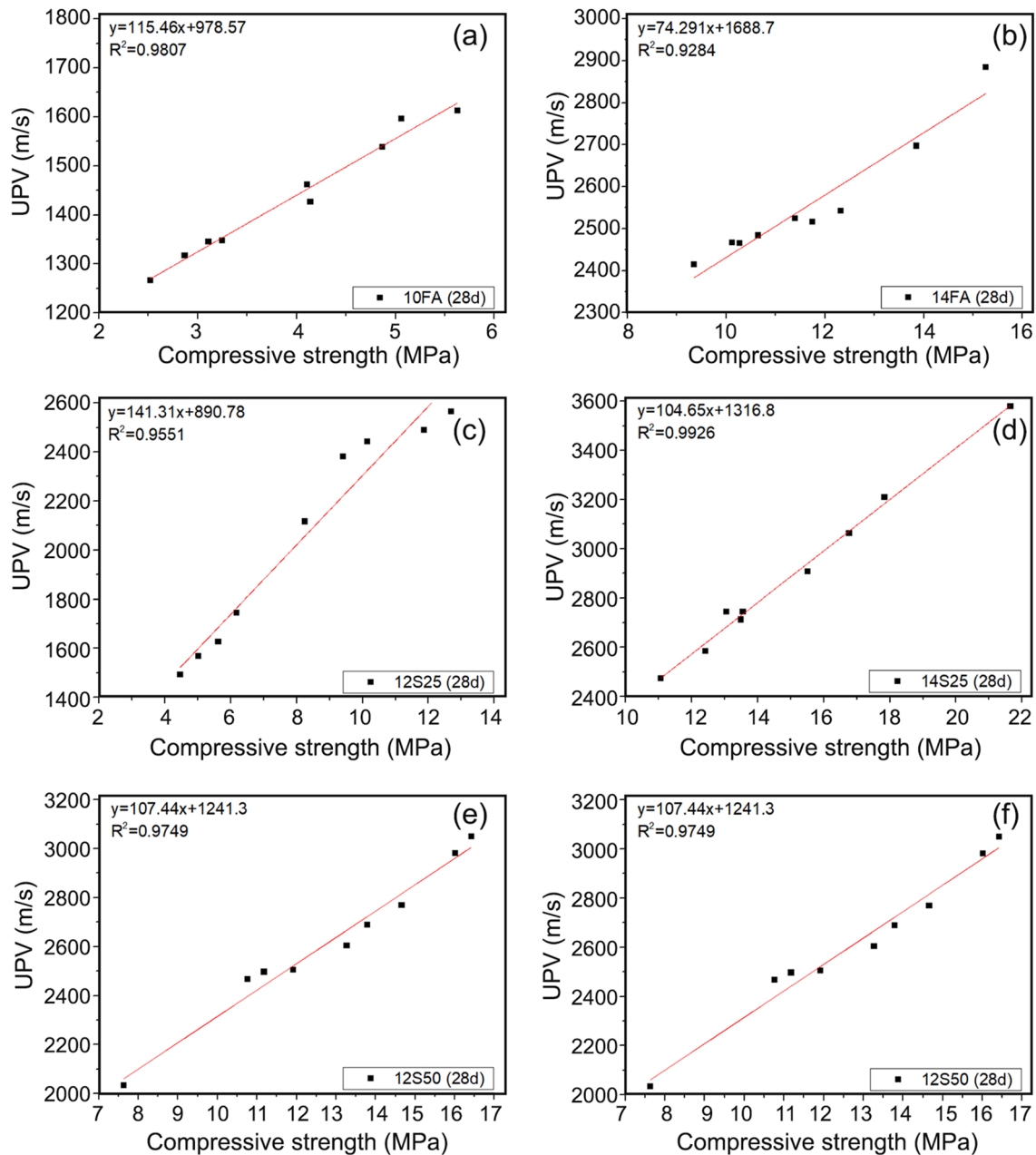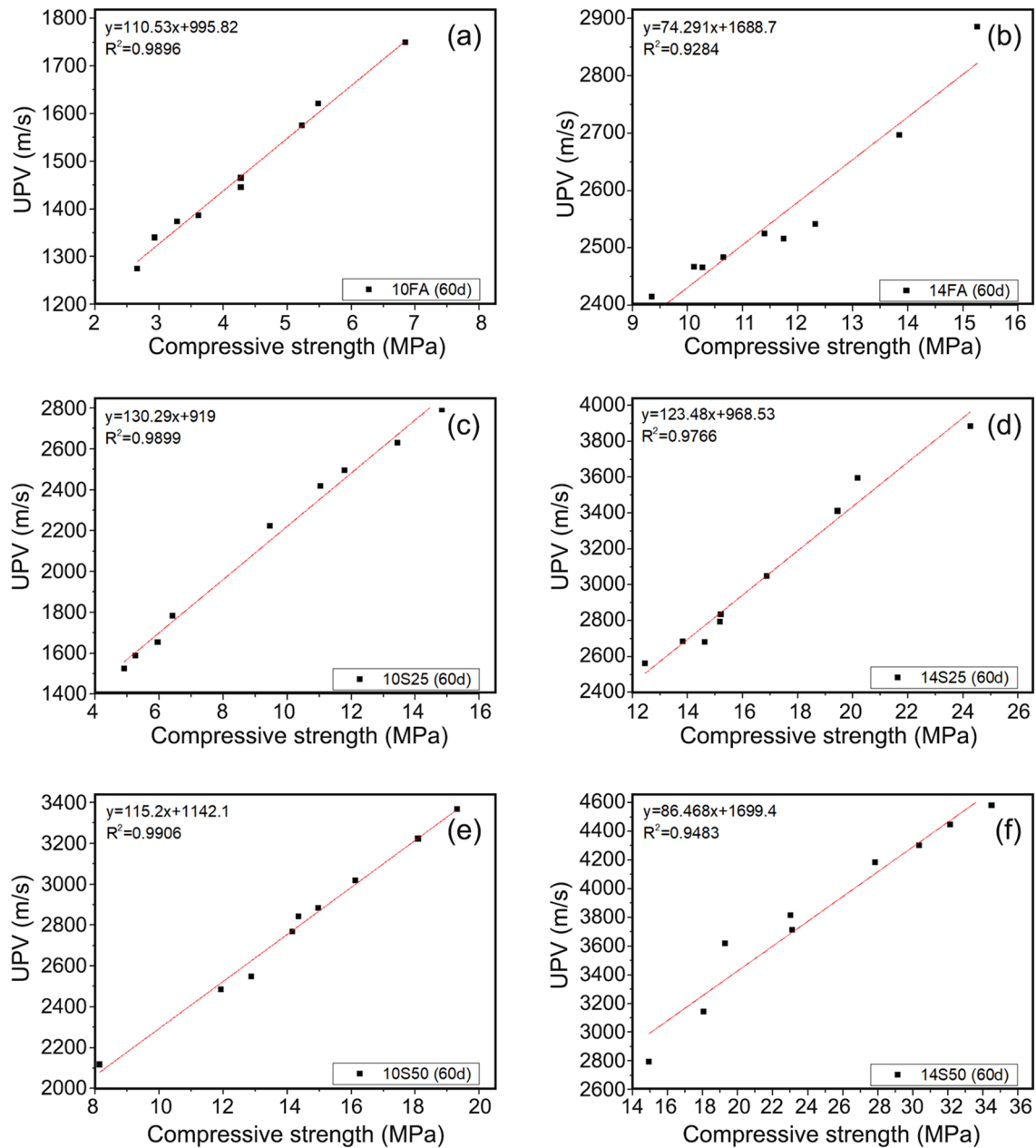
Fig. 9 Relationship between UPV and compressive strength for 28 day tests: **a** 10 M-100% FA, **b** 14 M-100% FA, **c** 10 M-25% GGBFS, **d** 14 M-25% GGBFS, **e** 10 M-50% GGBFS, and **f** 14 M-50% GGBFS

obtained in the group containing 100% AEFA. These ratios are 60.9% and 47.7% for the 14 M group, respectively. The highest increment for the 100% AEFA group is 28.6%. For 60 day results, similar increment ratios were obtained changing from 12.3% to 78.8% for all series.

When the changes that occur with the increase of the Ac/B ratio were examined, the highest values were obtained from the 0.65 ratio, just as in the compressive strength. In 28 day results, for 10 M 25% and 50% GGBFS-containing groups, the strength increment with the increases of Ac/B

ratio from 0.45 to 0.65 is 118% and 52.7%. For the 60 day series, these values are 120% and 92%, respectively. For 14 M 28 day tests, the highest increase for 100% AEFA, 25% GGBFS and 50% GGBFS groups, is 21.4%, 35% and 62.2%, respectively. These values are 26.4%, 40.9%, and 59.6, respectively, for the 60 day group.

It is possible to see that there is not a significant difference between the 28 day and 60 day values, but there is a slight increase in the 60 day values. In a study, researchers used SH solution between 8 and 16 M and examined the

Fig. 10 Relationship between UPV and compressive strength for 60 day tests **a** 10 M-100% FA, **b** 14 M-100% FA, **c** 10 M-25% GGBFS, **d** 14 M-25% GGBFS, **e** 10 M-50% GGBFS, and **f** 14 M-50% GGBFS

splitting tensile strength results of the high calcium-based geopolymers they produced. The values varied between 1.40–3.87 MPa for different molarity values [62]. In an article evaluating high calcium fly ash and silica resources, all the splitting tensile test results obtained when using 10, 12, and 14 M SH were below 4.5 MPa [48]. The values obtained in this study are compatible with those in the literature, and all values except three samples were below 4.5 MPa. It has been stated in the studies that the results are generally parallel to the results obtained in the compressive strength tests

[63]. The compressive and splitting tensile strength results in this study have the same trend. Therefore, it is thought that the factors affecting the changes in compressive strength results also affect the splitting tensile strength.

Scanning electron microscopy analysis

In order to investigate the microstructure of the geopolymers produced, scanning electron microscopy (SEM) analyses
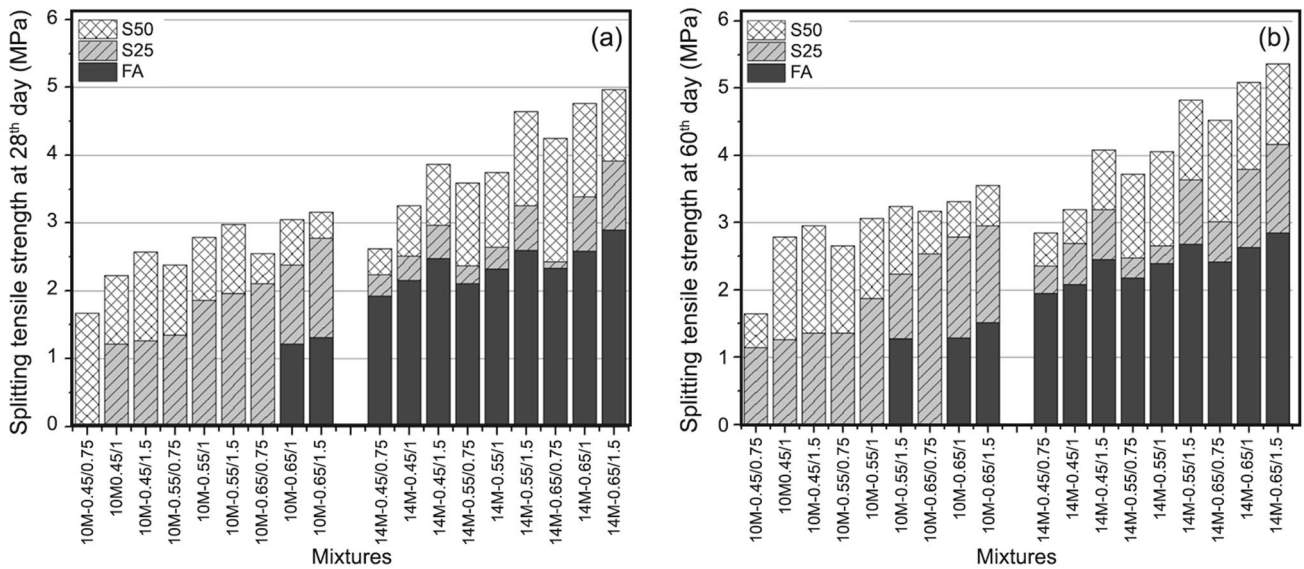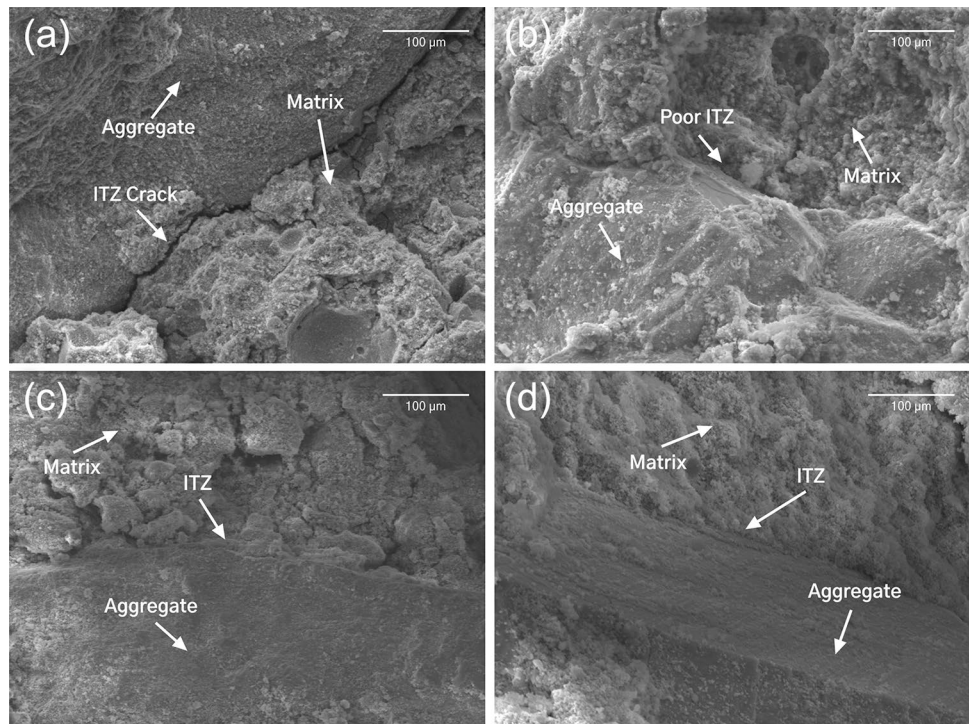
Fig. 11 Results of splitting tensile strength test: **a** 28 day, and **b** 60 day

Fig. 12 SEM images of the selected geopolymer samples: **a** 10FA-0.45/0.75, **b** 14FA-0.45/0.75, **c** 10S50-0.65/1.5 and **d** 14S50-0.65/1.5

were carried on. Figure 12 shows the SEM images of various 60 day samples.

Figure 12a belongs to the sample containing 10 M SH produced with 100% AEFA. From the figure, it can be seen that the matrix phase is quite loose and porous. At the same time, there is no sufficient interlocking between the aggregate particle and the matrix, and there is a large crack-like opening. When the SH concentration increased to 14 M

in the same sample (Fig. 12b), no major changes could be observed in the matrix phase. When the interfacial transition zone (ITZ) between aggregate and matrix is examined, it is seen that there is still a weak interlocking, but the significant gap between aggregate and matrix is not as clear as that shown in a Fig. 11a. From Fig. 11c it is seen that the aggregate matrix interface is in a much better condition when 50% GGBFS is added to the sample containing

10 M SH and SS/SH and Ac/B inceased to 1.5 and 0.65, respectively. In the matrix phase, an irregular and porous structure is observed. A regular, dense, and void-free matrix phase is seen when examining the sample using both 50% GGBFS and 14 M SH (Fig. 12d). At the same time, it can be said that the ITZ of the aggregate particle and the matrix is much more ideal when compared to other images. It is thought that the increase in the strength of the samples is due to this improvement between the aggregate and the matrix. At the same time, it is observed that there is a development in the matrix phase. For example, when the compressive strengths of the samples whose SEM images were investigated are examined, it is seen that they are 2.66, 9.53, 19.31, and 34.49 MPa, respectively. This may also be related to the presence of GGBFS in the structure. The reaction of the GGBFS and the alkaline solutions forms additional C–S–H and/or C–A–S–H gels and this leads to a denser and compacter microstructure [55, 64].

Conclusion

The effects of various geopolymerization parameters on the strength properties of AEFA-based geopolymers and GGBFS admixed geopolymers were experimentally investigated. According to the experimental study, the following conclusions can be drawn:

- Unit weights of 100% AEFA-containing geopolymers are lower than unit weights of conventional concrete but with the GGBFS addition these values came closer to the conventional concrete.
- 100% AEFA-based geopolymers have the lowest UPV results, and on the other hand, GGBFS incorporation increased the UPV results. 50% GGBFS-containing sample with 14 M SH, 0.65 Ac/B ratio, and 1.50 SS/SH ratio, has given the highest UPV result.
- With the increase of GGBFS, the compressive strength values increased. The highest strengths were obtained from 50% GGBFS groups. This can be related to the additional reactions of GGBFS. Compressive strength results increased with the increase of SS/SH and Ac/B ratio at all mixture groups.
- Splitting tensile strength results are similar to compressive strength results. These results also increased with the increase of GGBFS amount, SS/SH, and Ac/B ratio.
- The results indicated that AEFA, which has the highest waste reserve among the thermal power plant fly ashes in Turkey, was evaluated as partial geopolymer raw material. It can be seen that Afşin-Elbistan fly ash, which gave lower strength results by itself, can be evaluated by combining with GGBFS in various amounts. This combining may play an important role in utilizing the AEFA

which is not being preferable for the cement and concrete industry.

Data availability The data that support the findings of this study are available from the corresponding author upon reasonable request.

Declarations

Conflict of interest The authors declare that they have no known competing financial interests or personal relationships that could have appeared to influence the work reported in this paper.

References

1. Toniolo N, Boccaccini AR (2017) Fly ash-based geopolymers containing added silicate waste. a review. Ceram Int 43:14545–14551. https://doi.org/10.1016/j.ceramint.2017.07.221
2. Hadi MNS, Farhan NA, Sheikh MN (2017) Design of geopolymer concrete with GGBFS at ambient curing condition using taguchi method. Constr Build Mater 140:424–431. https://doi.org/10.1016/j.conbuildmat.2017.02.131
3. Mcnulty E (2009) Geopolymers: an environmental alternative to carbon dioxide producing ordinary portland cement. The Catholic University of America, Washington, D.C
4. Thokchom S, Ghosh P, Ghosh S (2012) Effect of Na_2O content on durability of geopolymer pastes in magnesium sulfate solution. Can J Civ Eng 39:34–43. https://doi.org/10.1139/l11-107
5. Rahier H, VanMele B, Wastiels J (1996) Low-temperature synthesized aluminosilicate glasses part II rheological transformations during low-temperature cure and high-temperature properties of a model compound. J Mater Sci 31:80–85. https://doi.org/10.1007/BF00355129
6. Palomo A, de la Fuente JIL (2003) Alkali-activated cementitious materials: alternative matrices for the immobilisation of hazardous wastes part I. Stab Boron Cem Concr Res 33:281–288. https://doi.org/10.1016/s0008-8846(02)00964-x
7. Mallicoat S, Sarin P, Kriven WM (2005). In: Briti ME, Filip P, Lewinsohn C, Sayir A, Opeka M, Mullins WM (eds) Developments in advanced ceramics and composites. The American Ceramic Society, Ohio
8. Sofi M, van Deventer JSJ, Mendis PA, Lukey GC (2007) Engineering properties of inorganic polymer concretes (IPCs). Cem Concr Res 37:251–257. https://doi.org/10.1016/j.cemconres.2006.10.008
9. Bao Y, Grutzeck MW, Jantzen CM (2005) Preparation and properties of hydroceramic waste forms made with simulated hanford

low-activity waste. J Am Ceram Soc 88:3287–3302. https://doi.org/10.1111/j.1551-2916.2005.00775.x

10. Reed M, Lokuge W, Karunasena W (2014) Fibre-reinforced geopolymer concrete with ambient curing for in situ applications. J Mater Sci 49:4297–4304. https://doi.org/10.1007/s10853-014-8125-3

11. Duxson P, Mallicoat SW, Lukey GC (2007) The effect of alkali and Si/Al ratio on the development of mechanical properties of metakaolin-based geopolymers. Coll Surf A Physicochem Eng Asp 292:8–20. https://doi.org/10.1016/j.colsurfa.2006.05.044

12 Kantarcı F (2022) Influence of fiber characteristics on sulfate resistance of ambient-cured geopolymer concrete. Struct Concr 23:775–790. https://doi.org/10.1002/suco.202100540

13. Aljanabi M, Çevik A, Niş A (2022) Residual mechanical performance of lightweight fiber-reinforced geopolymer mortar composites incorporating expanded clay after elevated temperatures. J Compos Mater 56:1737–1752. https://doi.org/10.1177/00219983221088902

14. Niş A, BilenlerAltundal M (2023) Durability performance of alkali-activated concretes exposed to sulfuric acid attack. Rev La constr 22:16–35. https://doi.org/10.7764/RDLC.22.1.16

15. Muñiz-Villarreal MS, Manzano-Ramírez A, Sampieri-Bulbarela S (2011) The effect of temperature on the geopolymerization process of a metakaolin-based geopolymer. Mater Lett 65:995–998. https://doi.org/10.1016/j.matlet.2010.12.049

16. Adak D, Sarkar M, Mandal S (2017) Structural performance of nano-silica modified fly-ash based geopolymer concrete. Constr Build Mater 135:430–439. https://doi.org/10.1016/j.conbuildmat.2016.12.111

17. Kupaei RH, Alengaram UJ, Jumaat MZ (2014) The effect of different parameters on the development of compressive strength of oil palm shell geopolymer concrete. Sci World J 2014:1–16. https://doi.org/10.1155/2014/898536

18. Feng J, Zhang R, Gong L et al (2015) Development of porous fly ash-based geopolymer with low thermal conductivity. Mater Des 65:529–533. https://doi.org/10.1016/j.matdes.2014.09.024

19. Barough AS, Shoubi MV, Kiani I, Amini Z. Advantages of using fly ash in concrete ındustry for achieving suistainable development. In: Management in construction research association (MICRA) post graduate conference.UTM Malaysia. 2010

20. Mallikarjuna Rao G, Gunneswara Rao TD (2015) Final setting time and compressive strength of fly ash and GGBS-based geopolymer paste and mortar. Arab J Sci Eng 40:3067–3074. https://doi.org/10.1007/s13369-015-1757-z

21. Nath P, Sarker PK (2014) Effect of GGBFS on setting, workability and early strength properties of fly ash geopolymer concrete cured in ambient condition. Constr Build Mater 66:163–171. https://doi.org/10.1016/j.conbuildmat.2014.05.080

22. Karakoç MB, Türkmen İ, Maraş MM (2014) Mechanical properties and setting time of ferrochrome slag based geopolymer paste and mortar. Constr Build Mater 72:283–292. https://doi.org/10.1016/j.conbuildmat.2014.09.021

23. Singh B, Ishwarya G, Gupta M, Bhattacharyya SK (2015) Geopolymer concrete: a review of some recent developments. Constr Build Mater 85:78–90. https://doi.org/10.1016/j.conbuildmat.2015.03.036

24. Heah CY, Kamarudin H, Al BAMM (2011) Effect of curing profile on kaolin-based geopolymers. Phys Procedia 22:305–311. https://doi.org/10.1016/j.phpro.2011.11.048

25. Rovnaník P (2010) Effect of curing temperature on the development of hard structure of metakaolin-based geopolymer. Constr Build Mater 24:1176–1183. https://doi.org/10.1016/j.conbuildmat.2009.12.023

26. NajafiKani E, Allahverdi A (2009) Effects of curing time and temperature on strength development of inorganic polymeric binder based on natural pozzolan. J Mater Sci 44:3088–3097. https://doi.org/10.1007/s10853-009-3411-1

27. Fernandes-Jiménez AM, Palomo A, Lopez-Hombrados C (2006) Engineering properties of compacted fly ash. ACI Mater J 103:106–112. https://doi.org/10.1061/JSFEAQ.0001744

28. Hardjito D, Wallah SE, Sumajouw DMJ, Rangan BV (2004) On the development of fly ash-based geopolymer concrete. ACI Mater J 101:467–472

29. Pan Z, Sanjayan JG, Rangan BV (2011) Fracture properties of geopolymer paste and concrete. Mag Concr Res 63:763–771. https://doi.org/10.1680/macr.2011.63.10.763

30. Diaz-Loya EI, Allouche EN, Vadiya S (2011) Mechanical properties of fly-ash-based geopolymer concrete. ACI Mater J 108:300–306

31. Niş A, Altındal İ (2021) Compressive strength performance of alkali activated concretes under different curing conditions. Period Polytech Civ Eng 65:556–565. https://doi.org/10.3311/PPci.17016

32. Zhang P, Gao Z, Wang J et al (2020) Properties of fresh and hardened fly ash/slag based geopolymer concrete: a review. J Clean Prod 270:122389. https://doi.org/10.1016/j.jclepro.2020.122389

33. Chi M, Huang R (2013) Binding mechanism and properties of alkali-activated fly ash/slag mortars. Constr Build Mater 40:291–298. https://doi.org/10.1016/j.conbuildmat.2012.11.003

34. Ruiz-Santaquiteria C, Skibsted J, Fernández-Jiménez A, Palomo A (2012) Alkaline solution/binder ratio as a determining factor in the alkaline activation of aluminosilicates. Cem Concr Res 42:1242–1251. https://doi.org/10.1016/j.cemconres.2012.05.019

35. Parveen SD, Junaid MT (2018) Mechanical and microstructural properties of fly ash based geopolymer concrete incorporating alccofine at ambient curing. Constr Build Mater 180:298–307. https://doi.org/10.1016/j.conbuildmat.2018.05.286

36. Mahyar M, Erdoğan ST (2015) Phosphate-activated high-calcium fly ash acid-base cements. Cem Concr Compos 63:96–103. https://doi.org/10.1016/j.cemconcomp.2015.09.002

37. Atiş CD, Kiliç A, Sevim UK (2004) Strength and shrinkage properties of mortar containing a nonstandard high-calcium fly ash. Cem Concr Res 34:99–102. https://doi.org/10.1016/S0008-8846(03)00247-3

38. Bicer A (2019) Influence of tragacanth resin on the thermal and mechanical properties of fly ash-cement composites. J Adhes Sci Technol 33:1019–1032. https://doi.org/10.1080/01694243.2018.1543530

39. DemirŞahin D, Çullu M, Eker H (2020) The effect of different fineness values of afşin elbistan fly ash on permeability in concrete. Chall J Struct Mech 6:73

40. Cinar M (2024) Utilization of earthquake demolition wastes and Afşin-Elbistan fly ash for soil improvement after the kahramanmaraş earthquake. Sustain 16:538. https://doi.org/10.3390/su16020538

41. Güneyli H (2010) Influence of Afşin-Elbistan highly limy fly ash on engineering behavior of a cohesive soil. Sci Res Essay 5:1307–1316

42. Erol M, Küçükbayrak S, Ersoy-Meriçboyu A (2007) Characterization of coal fly ash for possible utilization in glass production. Fuel 86:706–714. https://doi.org/10.1016/j.fuel.2006.09.009

43. Binici H, Aksogan O, Temiz H (2010) The use of fly ash and basaltic pumice as additives in the production of clay fired brick in Turkey. Int J Mater Res 101:887–893. https://doi.org/10.3139/146.110349

44. Bicer A (2021) The effect of fly ash and pine tree resin on thermo-mechanical properties of concretes with expanded clay aggregates. Case Stud Constr Mater 15:e00624. https://doi.org/10.1016/j.cscm.2021.e00624

45. Binici H, Gemci R, Kucukonder A, Solak HH (2012) Investigating sound insulation, thermal conductivity and radioactivity of chipboards produced with cotton waste, fly ash and barite. Constr

Build Mater 30:826–832. https://doi.org/10.1016/j.conbuildmat.2011.12.064

46. SeyedianChoubi S, MeralAkgul C (2022) High temperature exposure of alkali-activated coal fly ashes. J Build Eng 59:105081. https://doi.org/10.1016/j.jobe.2022.105081

47. Sarıdemir M, Bulut M, Deniz S, Deneme İÖ (2024) Long-term properties of steel fiber reinforced silica fume based AAMs at ambient and high temperatures. Constr Build Mater 416:135046. https://doi.org/10.1016/j.conbuildmat.2024.135046

48 Sevinç AH, Durgun MY (2020) Properties of high-calcium fly ash-based geopolymer concretes improved with high-silica sources. Constr Build Mater. https://doi.org/10.1016/j.conbuildmat.2020.120014

49. Şahin M, Mahyar M, Erdoğan ST (2016) Mutual activation of blast furnace slag and a high-calcium fly ash rich in free lime and sulfates. Constr Build Mater 126:466–475. https://doi.org/10.1016/j.conbuildmat.2016.09.064

50. Neville AM (1995) Properties of Concrete, 4th edn. Longman

51. Mehta PK, Monteiro PJM (2014) Concrete: microstructure, properties, and materials. McGraw-Hill Education, New York

52. Benaicha M, Jalbaud O, HafidiAlaoui A, Burtschell Y (2015) Correlation between the mechanical behavior and the ultrasonic velocity of fiber-reinforced concrete. Constr Build Mater 101:702–709. https://doi.org/10.1016/j.conbuildmat.2015.10.047

53. Phummiphan I, Horpibulsuk S, Rachan R (2018) High calcium fly ash geopolymer stabilized lateritic soil and granulated blast furnace slag blends as a pavement base material. J Hazard Mater 341:257–267. https://doi.org/10.1016/j.jhazmat.2017.07.067

54. Reddy MS, Dinakar P, Rao BH (2018) Mix design development of fly ash and ground granulated blast furnace slag based geopolymer concrete. J Build Eng 20:712–722. https://doi.org/10.1016/j.jobe.2018.09.010

55. De Filippis U, Prud'homme E, Meille S, (2021) Relation between activator ratio, hydration products and mechanical properties of alkali-activated slag. Constr Build Mater 266:120940. https://doi.org/10.1016/j.conbuildmat.2020.120940

56. Al Bakri Abdullah MM, Kamarudin H, Abdulkareem OAKA (2011) Optimization of alkaline activator/fly ashratio on the compressive strength of manufacturing fly ash-basedgeopolymer. Appl Mech Mater 110–116:734–739. https://doi.org/10.4028/www.scientific.net/AMM.110-116.734

57. Villa C, Pecina ET, Torres R, Gómez L (2010) Geopolymer synthesis using alkaline activation of natural zeolite. Constr Build Mater 24:2084–2090. https://doi.org/10.1016/j.conbuildmat.2010.04.052

58. Shariati M, Shariati A, Trung NT (2021) Alkali-activated slag (AAS) paste: correlation between durability and microstructural characteristics. Constr Build Mater 267:120886. https://doi.org/10.1016/j.conbuildmat.2020.120886

59. Gebregziabiher BS, Thomas R, Peethamparan S (2015) Very early-age reaction kinetics and microstructural development in alkali-activated slag. Cem Concr Compos 55:91–102. https://doi.org/10.1016/j.cemconcomp.2014.09.001

60. Ashrafian A, Taheri Amiri MJ, Rezaie-Balf M (2018) Prediction of compressive strength and ultrasonic pulse velocity of fiber reinforced concrete incorporating nano silica using heuristic regression methods. Constr Build Mater 190:479–494. https://doi.org/10.1016/j.conbuildmat.2018.09.047

61. Saint-Pierre F, Philibert A, Giroux B, Rivard P (2016) Concrete quality designation based on ultrasonic pulse velocity. Constr Build Mater 125:1022–1027. https://doi.org/10.1016/j.conbuildmat.2016.08.158

62. Lavanya G, Jegan J (2015) Evaluation of relationship between split tensile strength and compressive strength for geopolymer concrete of varying grades and molarity. Int J Appl Eng Res 10:35523–35529

63. Yan K, Xu H, Shen G, Liu P (2013) Prediction of splitting tensile strength from cylinder compressive strength of concrete by support vector machine. Adv Mater Sci Eng 2013:597257. https://doi.org/10.1155/2013/597257

64. Xu H, Gong W, Syltebo L (2014) Effect of blast furnace slag grades on fly ash based geopolymer waste forms. Fuel 133:332–340. https://doi.org/10.1016/j.fuel.2014.05.018

Authors and Affiliations

Ahmet Hayrullah Sevinç[1] · Muhammed Yasin Durgun[2]

✉ Ahmet Hayrullah Sevinç
ahmethayrullah.sevinc@istiklal.edu.tr

✉ Muhammed Yasin Durgun
mydurgun@bartin.edu.tr

[1] Elbistan Vocational School of Higher Education, Construction Program, Kahramanmaraş İstiklal University, 46300 Kahramanmaraş, Turkey

[2] Faculty of Engineering, Architecture and Design, Civil Engineering Department, Kutlubey-Yazıcılar Campus, Bartın University, 74100 Bartın, Turkey